

Full length article

Free vibration analysis of isogeometric curvilinearly stiffened shells

X.C. Qin^a, C.Y. Dong^{a,*}, F. Wang^b, Y.P. Gong^a^a School of Aerospace Engineering, Beijing Institute of Technology, Beijing 100081, China^b School of Information and Electronics, Beijing Institute of Technology, Beijing 100081, China

ARTICLE INFO

Keywords:

IGA

Curvilinearly stiffened shells

free vibration

ABSTRACT

The isogeometric analysis (IGA) proposed by Hughes is a new approach in which Non-Uniform Rational B-Splines (NURBS) are used as a geometric representation of an object. It has superiorities of capturing exact geometry, simplifying refinement strategy, easily achieving degree elevation with an arbitrary continuity of basic functions and getting higher calculation accuracy. In this paper, the IGA approach is extended to solve the free vibration problem of curvilinearly stiffened cylindrical and shallow shells. The first-order shear deformation theory (FSDT) and the Reissner-Mindlin shell theory are used to model the shells, and the three-dimensional curved beam theory is employed to model the stiffener which can be placed anywhere within the shell. Some numerical examples are solved to study the vibration behavior of the curvilinearly stiffened shells. The effects of shell and stiffener element numbers, boundary conditions, stiffener ply modes and shell thicknesses on the natural frequency are investigated. Results have shown the correctness and superiorities of the present method by comparing the results with those from commercial finite element software and some numerical methods in existing literatures. One of the advantages is that the element number is much less than commercial finite element software, whereas another is that the mesh refinement process is much more convenient compared with traditional finite element method (FEM).

1. Introduction

Stiffened shells have been widely used in aircraft fuselages, missile bodies, submarines and roofs for decades. These structures can achieve better stiffness and strength than normal shells as well as save the structure material and reduce the weight, which improve the utilization efficiency and economy.

During the last several decades, an increasing number of researches on stiffened shells have been conducted. Earlier studies on stiffened cylindrical shells using the finite element method (FEM) can be found in the paper of Hoppmann [1]. Orthogonal plate model was used to study the vibration of stiffened cylindrical shells where the stiffeners laid vertically. After that, Stanley and Ganesan [2] studied the free vibration of clamped stiffened cylindrical shells, in which both short and long shells were discussed, and the effects of stiffener type, number and laid form on the natural frequency were investigated. Additionally, Nayak and Bandyopadhyay [3] used the FEM to study the free vibration of several forms of stiffened shallow shells, including ellipsoidal, hyperboloid and conical shells. In order to study the free vibration of stiffened shell, Samanta and Mukhopadhyay [4] developed a three-node triangular shell element combining Kirchhoff triangular plate bending element with Allman plane stress element. Pan et al. [5] studied the free vibration of stiffened cylindrical shells under arbitrary

boundary conditions. Efimtsov and Lazarev [6] researched the forced vibration of stiffened plates and cylindrical shells. Recently, Balamurugan and Narayanan [7] studied the free vibration of stiffened piezoelectric plates and shells.

For the curvilinearly stiffened plates and shells, there already has been a number of work being completed based on FEM as well. Shi et al. [8,9] presented some researches on curvilinearly stiffened plates and shells using FEM, e.g. (1) the static, vibration and buckling analysis of curvilinearly stiffened plates; (2) the vibration with in-plane loading of curvilinearly stiffened plates; (3) the free vibration analysis of curvilinearly stiffened cylindrical shells. To study the stability behavior of complex shaped and multi-functional structure with the concept of integrated and bonded unitized structural components, Zhao and Kapania [10] proposed an efficient finite element buckling analysis of unitized stiffened composite panel stiffened by arbitrarily shaped stiffeners.

In addition to the FEM, a variety of other numerical methods have been widely applied to dynamic stiffened plates and shells. Li [11] gave a perturbed solution for the free vibration of ring-stiffened cylindrical shells. Cheng and Dade [12] used Gaussian spline collocation method to study the dynamic behavior of stiffened shells and plates. Mustafa and Ali [13] calculated the natural frequency of stiffened cylindrical shells using Ritz Method. Shi et al. [14] used Ritz Method to solve the

* Corresponding author.

vibration problem of curvilinearly stiffened shallow shells. Jafaria and Bagheri [15] studied the free vibration of ring-stiffened cylindrical shell. In their work, several methods were used, such as FEM, Ritz method and experimental approach. They discussed the influence of non-uniform rib section and non-equidistant rib laying problems. Qu et al. [16] analyzed the dynamic behavior of conical-cylindrical shells blessed with ring-stiffeners using a modified variational method in which a variety of boundary conditions were considered and the displacement trial functions were combined by Fourier polynomials and Chebyshev polynomials.

In this paper, the isogeometric analysis (IGA) method proposed by Hughes et al. [17] is applied for the free vibration of curvilinearly stiffened shells, which has not been presented in the literature to the authors' knowledge. The IGA has several advantages over standard FEM, e.g. the smoothness with arbitrary continuity order, exact representation of shapes even at the coarsest level of discretization, simple and systematic refinement strategy, and more accurate modeling of complex geometries can be easily obtained. In recent years, IGA has been used in many areas such as turbulence [18–20], fluid–structure interaction [21–23], incompressibility [24–26], structural analysis [27,28], shells [29] and phase-field analysis [30]. For structural mechanics, isogeometric analysis has been extensively studied for nearly incompressible linear and non-linear elasticity and plasticity problem [26], structural vibrations [28], the composite Reissner-Mindlin plates [31], Kirchhoff-Love shells [32–34], the large deformation with rotation-free [35] and structural shape optimization [36].

The first-order shear deformation theory (FSDT) and the Reissner-Mindlin shell theory are used to model the shells in this paper, and the three-dimensional curved beam theory is employed to model the stiffener. The free vibration behavior of curvilinearly stiffened shells is studied. The stiffeners can be placed anywhere within the shell. This paper is organized as follows: In Section 2, a brief introduction of the B-spline and NURBS basis functions is considered. After that, formulations of isogeometric analysis method are presented. In Section 3, the model of curvilinearly stiffened shells is set up. Then, free vibration analysis of the curvilinearly stiffened shells is carried out. Section 4 is devoted to numerical tests which show the performance of the proposed method. In Section 5, we close this paper with some conclusions. The code is written in the FORTRAN 90. Present results are compared with the results available and those obtained using the NASTRAN software.

2. Isogeometric analysis method

2.1. NURBS basis functions

Given a knot vector which is a sequence in a non-decreasing order of parameter values, written as $\{\xi_1, \xi_2, \dots, \xi_{n+p+1}\}$ ($\xi_i \leq \xi_{i+1}$, $i = 1, \dots, n+p$) where ξ_i is the i -th knot, n is the number of basis functions and p is the polynomial order. The associated B-spline basis functions for a given degree p , are defined recursively over the parametric domain by the knot vector. For $p = 0$ [17],

$$N_{i,0}(\xi) = \begin{cases} 1 & \text{if } \xi_i \leq \xi < \xi_{i+1} \\ 0 & \text{otherwise} \end{cases} \quad (1)$$

For $p \geq 1$

$$N_{i,p}(\xi) = \frac{\xi - \xi_i}{\xi_{i+p} - \xi_i} N_{i,p-1}(\xi) + \frac{\xi_{i+p+1} - \xi}{\xi_{i+p+1} - \xi_{i+1}} N_{i+1,p-1}(\xi) \quad (2)$$

The derivatives of B-spline basis functions can be got from lower order derivatives recursively. The first order derivative of a B-spline basis function is given by

$$\frac{d}{d\xi} N_{i,p}(\xi) = \frac{p}{\xi_{i+p} - \xi_i} N_{i,p-1}(\xi) - \frac{p}{\xi_{i+p+1} - \xi_{i+1}} N_{i+1,p-1}(\xi) \quad (3)$$

Derivative of the k -th order is

$$\frac{d^k}{d\xi^k} N_{i,p}(\xi) = \frac{p}{\xi_{i+p} - \xi_i} \left(\frac{d^{k-1}}{d\xi^{k-1}} N_{i,p-1}(\xi) \right) - \frac{p}{\xi_{i+p+1} - \xi_{i+1}} \left(\frac{d^{k-1}}{d\xi^{k-1}} N_{i+1,p-1}(\xi) \right) \quad (4)$$

B-splines are convenient for free-form modeling. However, it cannot exactly design some common geometries in engineering. To solve this problem one usually use NURBS which are the rational functions of B-splines.

NURBS basis functions are defined as [17].

$$R_{i,p}(\xi) = \frac{N_{i,p}(\xi) \omega_i}{\sum_{j=1}^n N_{j,p}(\xi) \omega_j} = \frac{N_{i,p}(\xi) \omega_i}{W(\xi)} \quad (5)$$

where $N_{i,p}(\xi)$ denotes the i -th B-spline basis function of order p and ω_i is the corresponding weight. For the special case in which $\omega_i = c$, $\forall i$, the NURBS basis reduces to the B-spline basis.

The first order derivative of a NURBS basis function is computed using the quotient rule. That is,

$$\frac{d}{d\xi} R_{i,p}(\xi) = \omega_i \frac{N_{i,p}'(\xi) W(\xi) - N_{i,p}(\xi) W'(\xi)}{W(\xi)^2} \quad (6)$$

where

$$W'(\xi) = \sum_{i=1}^n N_{i,p}'(\xi) \omega_i, \quad N_{i,p}' = \frac{dN_{i,p}}{d\xi} \quad (7)$$

2.2. Formulations for IGA

Take a two-dimensional element as an example to formulate isogeometric analysis method [37]. Referring to Fig. 1 for illustration, the mapping from the parametric domain to the physical domain is given by

$$\mathbf{x} = \sum_{I=1}^n R_I(\xi) \mathbf{P}_I \quad (8)$$

where $\mathbf{x} = (x(\xi), y(\xi))$, $\xi = (\xi, \eta)$, n is the number of the control points, R_I is the I -th shape function, \mathbf{P}_I is the I -th control point.

The Jacobian matrix of the geometry mapping is defined as

$$\mathbf{J}_\xi = \begin{bmatrix} x_{,\xi} & x_{,\eta} \\ y_{,\xi} & y_{,\eta} \end{bmatrix} \quad (9)$$

with the components calculated as

$$\begin{aligned} x_{,\xi} &= \sum_{i=1}^n R_{i,\xi} x_i, & x_{,\eta} &= \sum_{i=1}^n R_{i,\eta} x_i \\ y_{,\xi} &= \sum_{i=1}^n R_{i,\xi} y_i, & y_{,\eta} &= \sum_{i=1}^n R_{i,\eta} y_i \end{aligned} \quad (10)$$

where $R_{i,\xi}$ and $R_{i,\eta}$ are the derivatives of the i -th shape function R_i with respect to the parametric coordinates ξ and η respectively, x_i and y_i are the coordinates of the i -th control point respectively. The determinant of \mathbf{J}_ξ is denoted by $|\mathbf{J}_\xi|$.

The transformation from parent domain to a parametric domain $[\xi_i, \xi_{i+1}] \times [\eta_j, \eta_{j+1}]$ is given by

$$\begin{aligned} \xi &= \frac{1}{2}[(\xi_{i+1} - \xi_i)\bar{\xi} + (\xi_{i+1} + \xi_i)] \\ \eta &= \frac{1}{2}[(\eta_{j+1} - \eta_j)\bar{\eta} + (\eta_{j+1} + \eta_j)] \end{aligned} \quad (11)$$

where $\bar{\xi}$ and $\bar{\eta}$ represent the coordinates of Gauss point. Therefore, the determinant of the Jacobian of this transformation is

$$|\mathbf{J}_\xi| = \frac{1}{4}(\xi_{i+1} - \xi_i)(\eta_{j+1} - \eta_j) \quad (12)$$

So, integrals of a function f with two variations x and y over the physical domain can be computed as

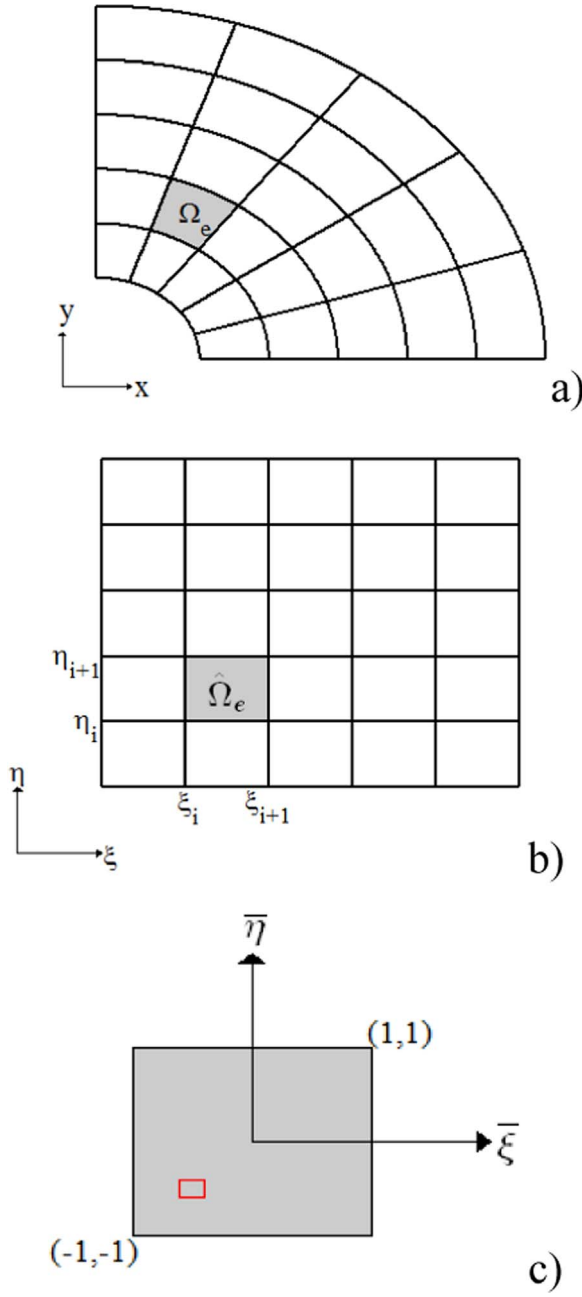


Fig. 1. Definition of domains used for integration in IGA: a) Physical domain; b) Parametric domain; c) Parent domain.

$$\begin{aligned}
 \int_{\Omega} f(x, y) d\Omega &= \sum_{e=1}^M \int_{\Omega_e} f(x, y) d\Omega_e = \sum_{e=1}^M \int_{\hat{\Omega}_e} f(x(\xi), y(\eta)) |J_{\xi}| d\hat{\Omega}_e \\
 &= \sum_{e=1}^M \int_{\square} f(x(\xi), y(\eta)) |J_{\xi}| |J_{\eta}| d\xi d\eta
 \end{aligned} \quad (13)$$

where Ω , Ω_e , $\hat{\Omega}_e$ and \square refer to the physical domain, the physical element, the parametric element and the parent element, respectively, as shown in Fig. 1; M is the number of elements in the entire geometry.

3. Formulations for curvilinearly stiffened shells

The curvilinearly stiffened shell modelled in a global coordinate system XYZ is shown in Fig. 2. The double-curved shell model is based on the Reissner-Mindlin shell theory and the first order shear deformation theory. And the stiffener is modelled in local coordinate system based on the Darboux coordinate system [38].

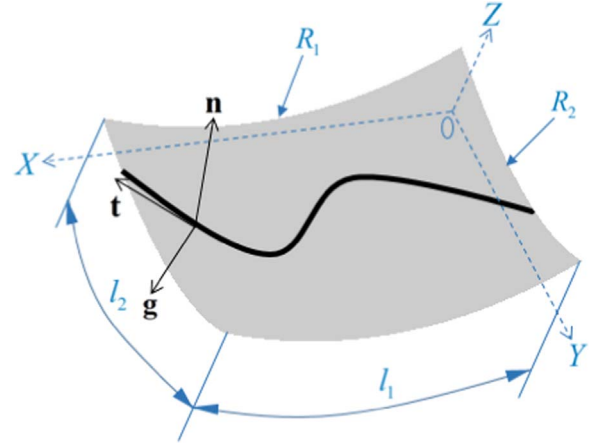


Fig. 2. Schematic of a curvilinearly stiffened shell.

3.1. Formulations for shell

Assuming that the mid-surface shell is defined in a local coordinate system xyz . The uniform thickness of the shell is h_s ; the radii of curvatures are R_1 and R_2 ; the edge lengths are l_1 and l_2 ; the displacements along x , y and z directions are u , v and w ; the rotations along y and x axes are β_x and β_y . Thus, the displacement field of the shell can be defined as

$$\mathbf{u}_s = [u, v, w, \beta_x, \beta_y]^T \quad (14)$$

Two special cases should be noted as follows.

- 1) The doubly-curved shell is shallow shell when the equation of the middle surface is $z = \frac{x^2}{2R_1} + \frac{y^2}{2R_2}$ and $\left(\frac{x}{R_1}\right)^2 \ll 1, \left(\frac{y}{R_2}\right)^2 \ll 1$.
- 2) The doubly-curved shell is cylindrical shell when $R_2 = \text{constant}$, $R_1 = \infty$ or $R_1 = \text{constant}$, $R_2 = \infty$.

Then, the displacement field of the shell can be written as

$$\mathbf{u}_s = \sum_{i=1}^n R_i(\xi, \eta) \mathbf{u}_{si} \quad (15)$$

where \mathbf{u}_{si} is the displacement vector of the i -th control point of the element.

The shell strain energy U_s and kinetic energy T_s can be respectively written as

$$U_s = \frac{1}{2} \iint_{\Omega} \boldsymbol{\varepsilon}_s^T \mathbf{D}_s \boldsymbol{\varepsilon}_s d\Omega = \frac{1}{2} \iint_{\Omega} \mathbf{u}_s^T \mathbf{B}_s^T \mathbf{D}_s \mathbf{B}_s \mathbf{u}_s d\Omega \quad (16)$$

$$T_s = \frac{1}{2} \iint_{\Omega} \dot{\mathbf{u}}_s^T \mathbf{m}_s \dot{\mathbf{u}}_s d\Omega \quad (17)$$

The kinematic relation between the strains $\boldsymbol{\varepsilon}_s$ and the displacements \mathbf{u}_s of the shell is

$$\boldsymbol{\varepsilon}_s = \mathbf{B}_s \mathbf{u}_s = \begin{pmatrix} \frac{\partial}{\partial x} & 0 & \frac{1}{R_x} & 0 & 0 \\ 0 & \frac{\partial}{\partial y} & \frac{1}{R_y} & 0 & 0 \\ \frac{\partial}{\partial y} & \frac{\partial}{\partial x} & 0 & 0 & 0 \\ 0 & 0 & 0 & \frac{\partial}{\partial x} & 0 \\ 0 & 0 & 0 & 0 & \frac{\partial}{\partial y} \\ 0 & 0 & 0 & \frac{\partial}{\partial y} & \frac{\partial}{\partial x} \\ -\frac{1}{R_x} & 0 & \frac{\partial}{\partial x} & 1 & 0 \\ 0 & -\frac{1}{R_y} & \frac{\partial}{\partial y} & 0 & 1 \end{pmatrix} \begin{pmatrix} u \\ v \\ w \\ \beta_x \\ \beta_y \end{pmatrix} = \begin{pmatrix} \varepsilon_x \\ \varepsilon_y \\ \gamma_{xy} \\ \kappa_x \\ \kappa_y \\ \kappa_{xy} \\ \gamma_{xz} \\ \gamma_{yz} \end{pmatrix} \quad (18)$$

The constitutive equation that relates stresses to strains for the shell is

$$\boldsymbol{\sigma}_s = \mathbf{D}_s \boldsymbol{\varepsilon}_s = \frac{E_s h_s}{1 - \nu^2} \begin{pmatrix} 1 & \nu & 0 & 0 & 0 & 0 & 0 & 0 \\ \nu & 1 & 0 & 0 & 0 & 0 & 0 & 0 \\ 0 & 0 & \frac{1-\nu}{2} & 0 & 0 & 0 & 0 & 0 \\ 0 & 0 & 0 & \frac{h_s^2}{12} & \nu \frac{h_s^2}{12} & 0 & 0 & 0 \\ 0 & 0 & 0 & \nu \frac{h_s^2}{12} & \frac{h_s^2}{12} & 0 & 0 & 0 \\ 0 & 0 & 0 & 0 & 0 & \frac{h_s^2(1-\nu)}{24} & 0 & 0 \\ 0 & 0 & 0 & 0 & 0 & 0 & K_g \frac{1-\nu}{2} & 0 \\ 0 & 0 & 0 & 0 & 0 & 0 & 0 & K_g \frac{1-\nu}{2} \end{pmatrix} \begin{pmatrix} \varepsilon_x \\ \varepsilon_y \\ \gamma_{xy} \\ \kappa_x \\ \kappa_y \\ \kappa_{xy} \\ \gamma_{xz} \\ \gamma_{yz} \end{pmatrix} \quad (19)$$

where E_s is Young's modulus, ν is Poisson's ratio, K_g is shearing correction factor.

The mass matrix of the shell is

$$\mathbf{m}_s = \rho_s \begin{pmatrix} h_s & 0 & 0 & 0 & 0 \\ 0 & h_s & 0 & 0 & 0 \\ 0 & 0 & h_s & 0 & 0 \\ 0 & 0 & 0 & h_s^3/12 & 0 \\ 0 & 0 & 0 & 0 & h_s^3/12 \end{pmatrix} \quad (20)$$

where ρ_s is the density of the shell.

3.2. Formulations for stiffener

Assuming that the 3D stiffener is made of a kind of homogeneous, isotropic and linear elastic material. The local coordinate system, known as Darboux coordinate system, is consist of the tangent direction \mathbf{t} , the principle normal direction \mathbf{n} and the geodesic direction \mathbf{g} , as shown in Fig. 2.

Let stiffener's displacement field be

$$\mathbf{u}_b = [u_t, u_g, u_n, \beta_t, \beta_g]^T \quad (21)$$

where u_t , u_g and u_n are the displacements along \mathbf{t} , \mathbf{g} and \mathbf{n} directions, β_t and β_g are the rotations along g and t axes.

Then, the displacement of stiffener can be written as

$$\mathbf{u}_b = \sum_{i=1}^l R_i(\zeta) \mathbf{u}_{bi} \quad (22)$$

where \mathbf{u}_{bi} is the displacement vector of the i -th control point of the stiffener element, l is the number of control points.

The length of the stiffener can be calculated with natural coordinates as

$$J = \int_{-1}^1 J d\zeta \quad (23)$$

where $J = \|\mathbf{r}_b'\|$ is the Jacobian conversion, \mathbf{r}_b is the coordinate vector of a point on the stiffener, and \mathbf{r}_b' is the derivative of \mathbf{r}_b with respect to the natural coordinate ζ .

The curvature K_n , principal curvature K_p and geodesic curvature K_g can be got from the following formula [38].

$$K_n = \frac{L \left(\frac{dx}{d\zeta} \right)^2 + 2M \left(\frac{dx}{d\zeta} \right) \left(\frac{dy}{d\zeta} \right) + N \left(\frac{dy}{d\zeta} \right)^2}{E \left(\frac{dx}{d\zeta} \right)^2 + 2F \left(\frac{dx}{d\zeta} \right) \left(\frac{dy}{d\zeta} \right) + G \left(\frac{dy}{d\zeta} \right)^2}$$

$$K_p = \frac{1}{R_p} = \frac{\|\mathbf{r}_b' \times \mathbf{r}_b''\|}{\|\mathbf{r}_b'\|^3}$$

$$K_g^2 = K_p^2 - K_n^2 \quad (24)$$

Detailed expressions of L , M , N , E , F and G of the above formula can be found in [38].

The stiffener strain energy U_b and kinetic energy T_b can be respectively written as:

$$U_b = \frac{1}{2} \int_{\Gamma} \boldsymbol{\varepsilon}_b^T \mathbf{D}_b \boldsymbol{\varepsilon}_b d\Gamma = \frac{1}{2} \int_{\Gamma} \mathbf{u}_b^T \mathbf{B}_b^T \mathbf{D}_b \mathbf{B}_b \mathbf{u}_b d\Gamma \quad (25)$$

$$T_b = \frac{1}{2} \int_{\Gamma} \dot{\mathbf{u}}_b^T \mathbf{m}_b \dot{\mathbf{u}}_b d\Gamma \quad (26)$$

The kinematic relation between strains $\boldsymbol{\varepsilon}_b$ and the displacements \mathbf{u}_b of the stiffener is

$$\boldsymbol{\varepsilon}_b = \mathbf{B}_b \mathbf{u}_b = \begin{pmatrix} \frac{1}{J} \frac{\partial}{\partial \zeta} & \frac{1}{R_g} & -\frac{1}{R_n} & 0 & 0 \\ 0 & \frac{1}{J} \frac{\partial}{\partial \zeta} & 0 & 0 & 0 \\ -\frac{1}{R_n} & 0 & \frac{1}{J} \frac{\partial}{\partial \zeta} & 1 & 0 \\ 0 & 0 & 0 & \frac{1}{J} \frac{\partial}{\partial \zeta} & 0 \\ 0 & 0 & 0 & 0 & \frac{1}{J} \frac{\partial}{\partial \zeta} \end{pmatrix} \begin{pmatrix} u_t \\ u_g \\ u_n \\ \beta_t \\ \beta_g \end{pmatrix} = \begin{pmatrix} \varepsilon_t \\ \gamma_n \\ \gamma_g \\ \kappa_t \\ \kappa_g \end{pmatrix} \quad (27)$$

The constitutive equation that relates stresses to strains for the stiffener is

$$\boldsymbol{\sigma}_b = \mathbf{D}_b \boldsymbol{\varepsilon}_b = \begin{pmatrix} E_b A_b & 0 & 0 & E_b A_b e & 0 \\ 0 & G_b A_g & 0 & 0 & 0 \\ 0 & 0 & G_b A_n & 0 & 0 \\ E_b A_b e & 0 & 0 & E_b J_g & 0 \\ 0 & 0 & 0 & 0 & G_b J_t \end{pmatrix} \begin{pmatrix} \varepsilon_t \\ \gamma_n \\ \gamma_g \\ \kappa_t \\ \kappa_g \end{pmatrix} \quad (28)$$

where E_b is Young's modulus, $G_b = E_b/2(1 + \nu)$ is shear modulus, e is eccentricity factor, $A_g = \kappa_g A_b$ and $A_n = \kappa_n A_b$ are the shearing areas corresponding to directions \mathbf{g} and \mathbf{n} respectively, $A_b = w_b h_b$ is cross-sectional area, w_b and h_b are the width and height respectively, κ_g and κ_n are the shearing correction factors corresponding to directions \mathbf{g} and \mathbf{n} respectively, J_g is the second moment of area A_g , J_t is the torque of cross-sectional area and $J_t = h_f b_f^3/3$ for rectangular stiffener.

The mass matrix of the stiffener is

$$\mathbf{m}_b = \rho_b \begin{pmatrix} A_b & 0 & 0 & A_b e & 0 \\ 0 & A_b & 0 & 0 & 0 \\ 0 & 0 & A_b & 0 & 0 \\ A_b e & 0 & 0 & I_n & 0 \\ 0 & 0 & 0 & 0 & I_n + I_b \end{pmatrix} \quad (29)$$

where ρ_b is the density of the stiffener.

To build the equation of stiffened cylindrical shells, displacement field should be unified. In this paper, we change the displacement field of the stiffener into that of the shell. The displacement filed for the stiffener can be approximated by that for the shell where a stiffener is located. Thus, we have the displacement filed for the stiffener

$$\mathbf{u}_b = \mathbf{T} \mathbf{u}_s = \mathbf{T} \sum_{j=1}^l R_j \sum_{i=1}^n R_i \mathbf{u}_{si} = \mathbf{T} \mathbf{N}_{sb} \mathbf{u}_s \quad (30)$$

where l and n are the numbers of the control points of the stiffener element and shell element respectively. The transformation matrix is

$$\mathbf{T} = \begin{pmatrix} \cos \alpha & \sin \alpha & 0 & 0 & 0 \\ -\sin \alpha & \cos \alpha & 0 & 0 & 0 \\ 0 & 0 & 1 & 0 & 0 \\ 0 & 0 & 0 & \cos \alpha & \sin \alpha \\ 0 & 0 & 0 & -\sin \alpha & \cos \alpha \end{pmatrix} \quad (31)$$

in which α is the angle between the stiffener tangential direction \mathbf{t} and x axis mentioned in Section 3.1, which is calculated at the Gaussian integration point, i.e.

$$\cos \alpha = \frac{x_s'}{J}; \quad \sin \alpha = \frac{y_s'}{J} \quad (32)$$

The numerator means the first order derivative with respect to the stiffener arch length. J is the determinant of the Jacobian matrix.

Finally, we can rewrite the stiffener strain energy and kinetic energy as follows

$$U_b = \frac{1}{2} \int_{\Gamma} \mathbf{u}_s^T \mathbf{N}_{sb}^T \mathbf{T}^T \mathbf{B}_b^T \mathbf{D}_b \mathbf{B}_b \mathbf{T} \mathbf{N}_{sb} \mathbf{u}_s d\Gamma \quad (33)$$

$$T_b = \frac{1}{2} \int_{\Gamma} \dot{\mathbf{u}}_s^T \mathbf{N}_{sb}^T \mathbf{T}^T \mathbf{m}_b \mathbf{T} \mathbf{N}_{sb} \dot{\mathbf{u}}_s d\Gamma \quad (34)$$

3.3. The weak form of the curvilinearly stiffened shells

Hamilton's principle is employed to derive the weak form of the governing equation for the stiffened shells.

$$\int_{t_1}^{t_2} [(\delta U_s + \delta U_b) + (\delta G_s + \delta G_b) - (\delta T_s + \delta T_b) - \delta W] dt = 0 \quad (35)$$

where δ is the symbol of variation, W is the work done by the external forces, G_s and G_b are the geometric strain energies of the shell and the stiffener respectively, t_1 and t_2 are the start and end times respectively.

For the free vibration analysis, the work of external forces and the geometric strain energy can be omitted. The principle expression can be expressed as

$$\int_{t_1}^{t_2} \left[\iint_{\Omega} \delta \mathbf{u}_s^T (\mathbf{B}_s^T \mathbf{D}_s \mathbf{B}_s) \mathbf{u}_s dS + \int_{\Gamma} \delta \mathbf{u}_s^T (\mathbf{N}_{sb}^T \mathbf{T}^T \mathbf{B}_b^T \mathbf{D}_b \mathbf{B}_b \mathbf{T} \mathbf{N}_{sb}) \mathbf{u}_s d\Gamma - \iint_{\Omega} \delta \mathbf{u}_s^T \mathbf{m}_s \ddot{\mathbf{u}}_s dS - \int_{\Gamma} \delta \mathbf{u}_s^T (\mathbf{N}_{sb}^T \mathbf{T}^T \mathbf{m}_b \mathbf{T} \mathbf{N}_{sb}) \ddot{\mathbf{u}}_s d\Gamma \right] dt = 0 \quad (36)$$

The formulation above can also be written as

$$(\mathbf{K} - \omega^2 \mathbf{M}) \mathbf{d} = 0 \quad (37)$$

where \mathbf{K} and \mathbf{M} are the stiffness and mass matrices of the stiffened shell respectively, ω is the angular frequency, \mathbf{d} is vector of the total displacement filed of shell.

4. Results and discussions

In this section, several numerical examples are exhibited to analyze the curvilinearly stiffened shells.

4.1. Analysis for curvilinearly stiffened cylindrical shells

Shi et al. [9] studied the free vibration of the model as shown in Fig. 3 using FEM. It is a simply supported cylindrical shell with an eccentric stiffener on it. The material and geometric properties are: $E = 73\text{GPa}$, $\rho = 2837\text{kg/m}^3$, $\nu = 0.33$, $R_1 = 100\text{mm}$, $R_2 = \infty$, $l_2 = 400\text{mm}$, $h_s = 1.5\text{mm}$, $h_b = 10\text{mm}$, $w_b = 2\text{mm}$.

In this example, a quartic NURBS mesh for shell is used and the numbers of shell elements and stiffener elements can be changed. The initial control points, weights and knot vectors are given in Appendix A. We change the refinement number to get the elements needed and the corresponding control points and weights can be computed.

For the given numbers of elements of the shell and stiffener, the natural frequencies are investigated. Results are compared with those from FEM [9], as shown in Table 1.

It is found that the frequencies are convergent and the error is very small when 27×27 shell elements and 27 stiffener elements are used.

Now, the number of the stiffener elements is fixed to 27. The corresponding natural frequencies are calculated by using different numbers of shell elements.

The results in Table 2 show that the number of shell elements has a great influence on natural frequencies. When the shell elements are few (e.g. 4×4), the error of the natural frequencies is unacceptable.

Similarly, the number of the shell elements is fixed to 27×27 . The corresponding natural frequencies are calculated by using different numbers of stiffener elements.

The results in Table 3 show that the number of stiffener elements has a small influence on natural frequencies. As a whole, the natural frequencies are smaller when the fewer stiffener elements are taken.

In summary, it is reasonable to take the number of the cylindrical

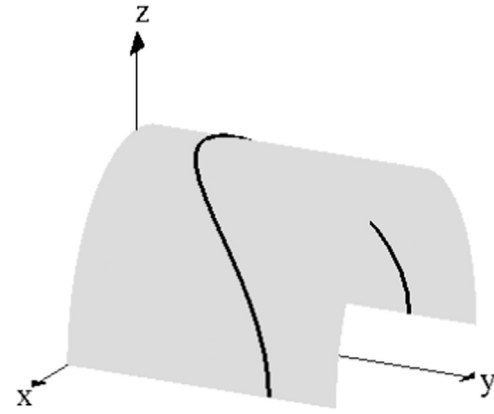


Fig. 3. Curvilinearly stiffened cylindrical shell.

Table 1

First ten natural frequencies (Hz) of a shell with a curvilinearly stiffener.

Mode	Element number					FEM [9]
	NS	4 × 4	8 × 8	16 × 16	27 × 27	
	NF	4	8	16	27	29
1		1899	1406	1380	1297	1295
2		2092	1423	1392	1404	1404
3		2677	1956	1956	1833	1828
4		3417	2152	2018	1973	1972
5		3671	2367	2251	2088	2085
6		4096	2596	2503	2342	2339
7		4226	2717	2625	2622	2617
8		4431	2754	2673	2627	2625
9		5136	2992	2875	2657	2652
10		5341	3509	3002	2803	2799

NS: Shell element number; NF: Stiffener element number

shell elements and stiffener elements as 27×27 and 27 respectively. When analyzing with Nastran, the number of shell elements is 5426 and that of stiffener elements is 180 which are much more than the IGA method. So, it can be concluded that the IGA can provide good results using fewer elements compared with Nastran.

To verify natural frequency, it is necessary to carry out mode shape identification. The first six mode shapes obtained by the IGA are compared with the results from FEM [9], as shown in Fig. 4. Obviously, the first six mode shapes are in good agreement with those from FEM.

As a more general example, a cylindrical shell with three arbitrary stiffeners is studied, as can be seen in Fig. 5. The boundary conditions are clamped at all edges. Except for the height for the shell and the geometrical parameters of the stiffener, all the other material parameters are unchanged. The height is changed into $l_2 = 200\text{mm}$, and the

Table 2

First ten natural frequencies (Hz) of a shell with a curvilinearly stiffener when the stiffener element number is fixed to 27.

Mode	Shell element number (NS)			
	4 × 4	8 × 8	16 × 16	27 × 27
1	1929	1447	1396	1297
2	2119	1462	1400	1404
3	2877	2083	1970	1833
4	3527	2243	2046	1973
5	3645	2569	2288	2088
6	4170	2621	2523	2342
7	4275	2835	2638	2622
8	4470	2897	2681	2627
9	5127	3218	2905	2657
10	5395	3533	3058	2803

Table 3

First ten natural frequencies (Hz) of a shell with a curvilinearly stiffener when the shell element number is fixed to 27×27 .

Mode	Stiffener element number (NF)			
	4	8	16	27
1	1231	1284	1296	1297
2	1376	1385	1402	1404
3	1748	1818	1831	1833
4	1918	1944	1968	1973
5	1944	1998	2070	2088
6	2144	2248	2330	2342
7	2517	2551	2615	2622
8	2624	2594	2622	2627
9	2655	2661	2669	2657
10	2737	2709	2772	2803

geometrical parameters of the stiffeners are $h_s = 1.5\text{mm}$, $h_b = 10\text{mm}$, $w_b = 2\text{mm}$. The control points, weights and knot vectors are given in Appendix B.

The first six mode shapes and natural frequencies obtained by Nastran and present method are given in Fig. 6. Considering that the number of stiffener elements has a small influence on natural frequencies and to save the computational time, the shell element number is chosen to be 27×27 and the stiffener element number is 19 instead of 27 in this example. As is seen from Fig. 6, both the natural frequencies and shape modes match well with Nastran and FEM [9].

4.2. Analysis for curvilinearly stiffened shallow shells

A clamped shallow shell as shown in Fig. 7 is considered. It has an eccentric stiffener on it. The material and geometric properties are $E = 73\text{GPa}$, $\rho = 2837\text{kg/m}^3$, $\nu = 0.33$, $l_1 = l_2 = 1569.8\text{mm}$, $R_1 = R_2 =$

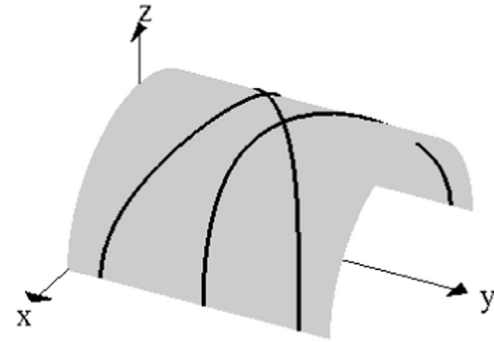


Fig. 5. A general cylindrical shell with three arbitrary stiffeners.

100mm , $h_s = 12.5\text{mm}$, $h_b = 44.8\text{mm}$, $w_b = 8.12\text{mm}$. In this example, a quadratic NURBS mesh is used for shell. The initial control points, weights and knot vectors are given in Appendix C.

For the given numbers of elements of the shell and stiffener, the natural frequencies are investigated. Results are compared with those from Nastran and Ritz Method [14], as shown in Table 4. The frequencies verify the convergence and accuracy of the IGA method. Besides, it can be found that the frequencies are convergent and the error between IGA method and either Nastran or FEM is very small when 18×18 shell elements and 18 stiffener elements are used.

Then, the number of the stiffener elements is fixed to 18. The corresponding natural frequencies are calculated by using different numbers of shell elements. Similar to the case of the curvilinearly stiffened cylindrical shells, the results indicate that the number of shell elements has a great influence on natural frequencies, as shown in Table 5. When the shell elements are few (e.g. 4×4), the error is unacceptable.

Afterwards, the number of the shell elements is fixed to 18×18 . The

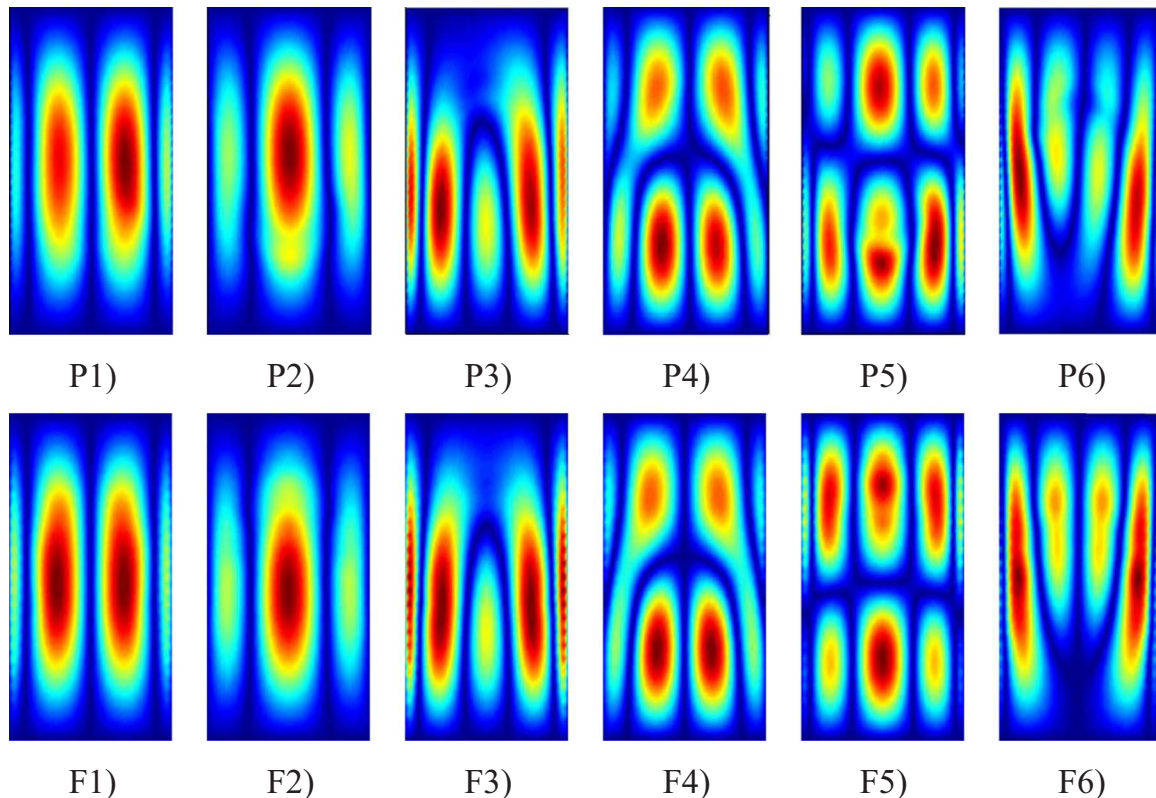


Fig. 4. First six mode shape comparison for a curvilinearly stiffened cylindrical shell, i.e. P1)-P6): present results; F1)-F6): FEM results.

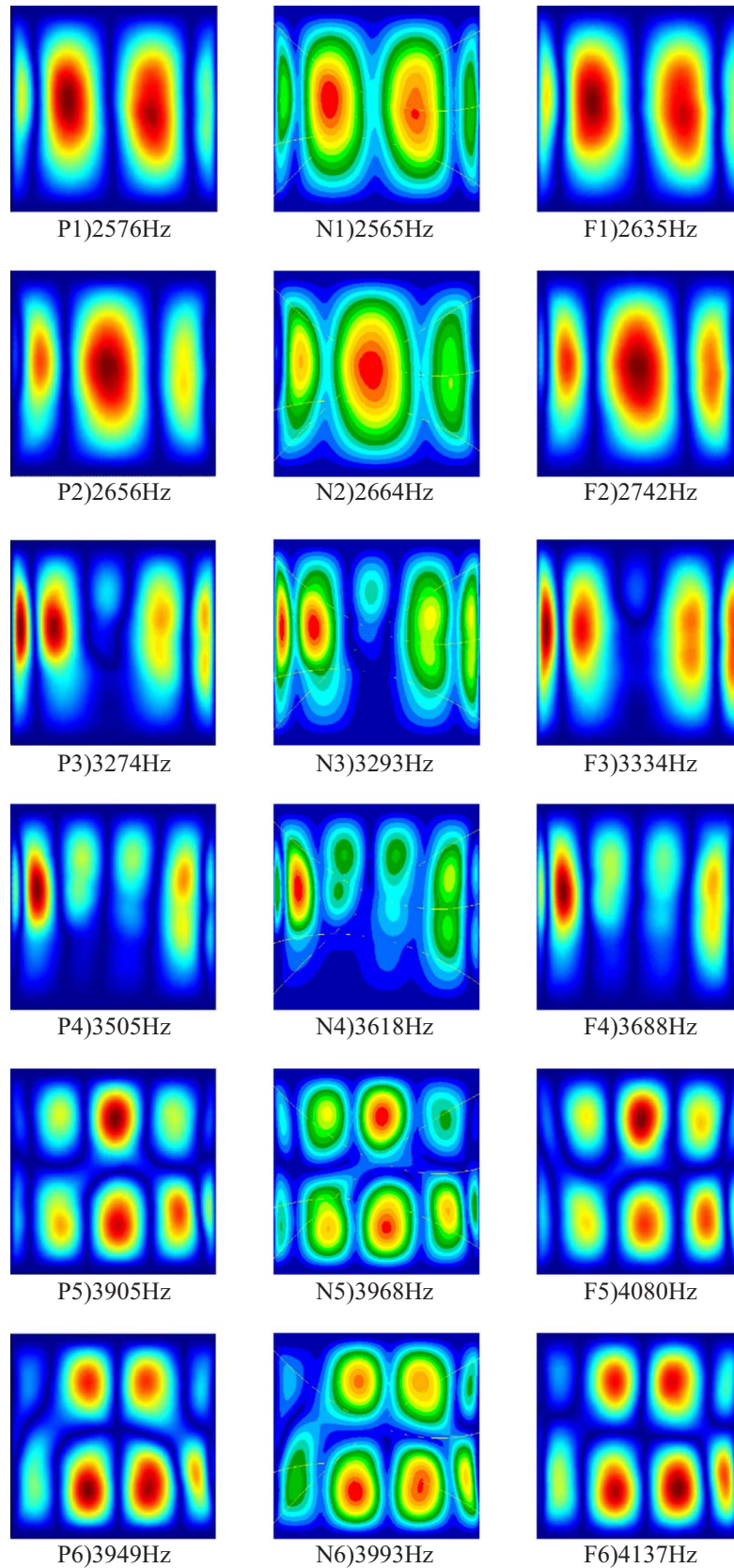


Fig. 6. First six mode shape and natural frequency comparison, i.e. P1)–P6): Present results; N1)–N6): Nastran results; F1)–F6): FEM results.

natural frequencies are calculated by using different numbers of stiffener elements. The results in Table 6 indicate that the number of stiffener elements has a small effect on natural frequencies.

Consequently, it is reasonable to take the number of the shallow

shell elements and stiffener elements as 18×18 and 18 respectively.

In this example, when analyzing with Nastran, the number of shell elements is 1584 and that of stiffener elements is 50 which are much more than the IGA method too.

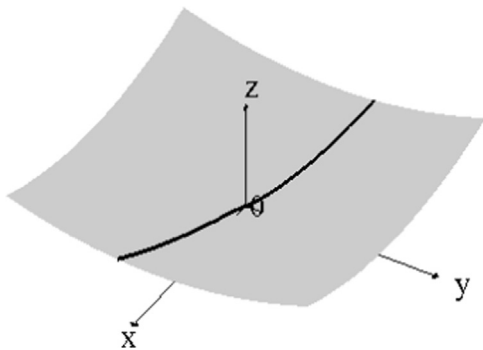


Fig. 7. A curvilinearly stiffened shallow shell.

Table 4
First ten natural frequencies (Hz) of a shallow shell with a curvilinearly stiffener.

Mode	Element number						Nastran	Ritz [14]
	NS	4 × 4	8 × 8	16 × 16	18 × 18	27 × 27		
	NF	4	8	16	18	27		
1		470	368	339	338	338	342	336
2		630	375	350	348	347	343	340
3		706	431	367	363	362	346	344
4		832	445	373	370	368	365	373
5		1867	472	380	376	375	366	379
6		1876	480	390	388	387	392	405
7		1884	518	410	402	399	395	409
8		1914	570	443	436	435	416	431
9		1976	657	444	439	438	428	443
10		1998	801	460	452	449	430	451

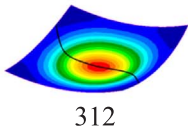
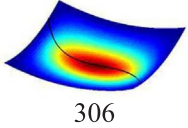
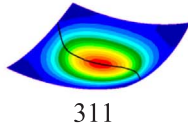
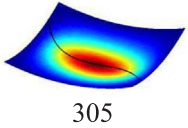
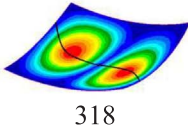
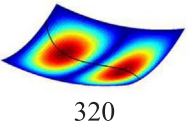
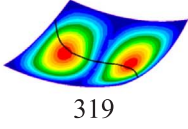
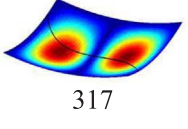
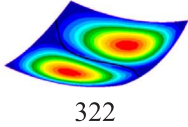
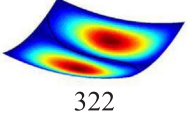
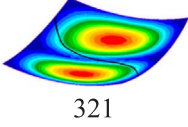
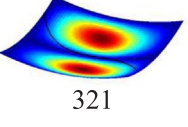
Table 5
First ten natural frequencies (Hz) of a shell with a curvilinearly stiffener when the stiffener element number is fixed to 18.

Mode	Shell element number (NS)			
	4 × 4	8 × 8	16 × 16	18 × 18
1	472	368	339	338
2	645	376	350	348
3	745	432	367	363
4	859	447	373	370
5	1867	476	380	376
6	1876	483	390	388
7	1892	518	411	402
8	1946	581	443	436
9	1974	683	445	439
10	2008	803	460	452

Table 6
First ten natural frequencies (Hz) of a shell with a curvilinearly stiffener when the shell element number is fixed to 18 × 18.

Mode	Stiffener element number (NF)			
	4	8	16	18
1	340	338	338	338
2	345	347	348	348
3	360	363	363	363
4	362	366	369	370
5	371	375	376	376
6	384	387	388	388
7	393	398	402	402
8	420	433	436	436
9	427	434	439	439
10	441	447	451	452

Table 7
Natural frequencies (Hz) and mode shapes of a simply supported stiffened shallow shell.

Mode	Concentrically		Eccentrically	
	Nastran	Present	Nastran	Present
1	 312	 306	 311	 305
2	 318	 320	 319	 317
3	 322	 322	 321	 321

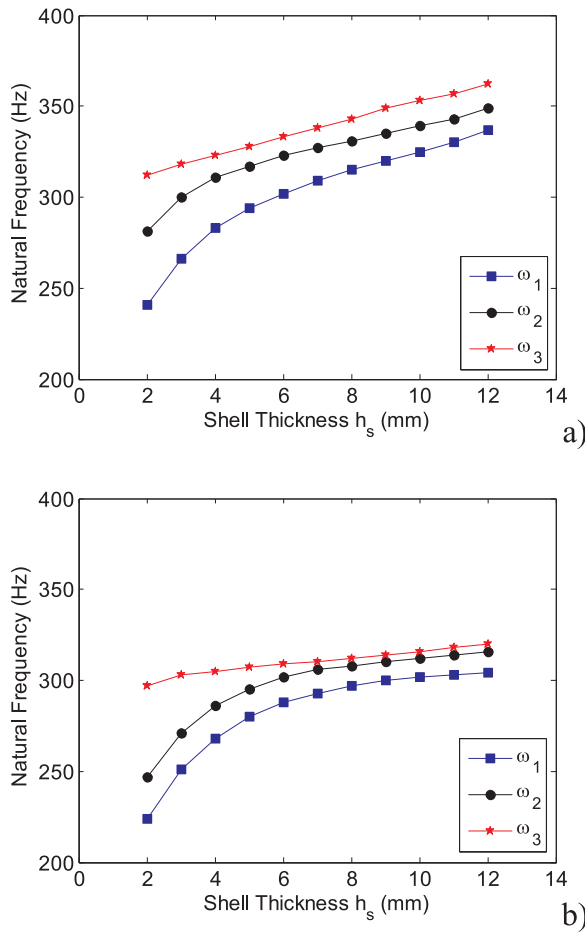


Fig. 8. The relationship between natural frequency and shell thickness: a) clamped condition; b) simply supported condition.

To review the effect of the ply mode on the natural frequency, we study a simply supported shallow shell with concentric and eccentric stiffener respectively. The natural frequencies and shape modes are compared with those gained by Nastran simulation, as shown in Table 7. Here, we use 18×18 shell elements and 18 stiffener elements.

Appendix A

The two initial shell element knot vectors (one for each direction) are both $\{0, 0, 0, 0, 0, 1, 1, 1, 1, 1\}$. The initial knot vector of the stiffener is $\{0, 0, 0, 0, 0, 0.25, 0.5, 0.75, 1, 1, 1, 1, 1\}$. The initial control points and weights are listed in Table 8.

Table 8
The coordinates of control points and weights in Fig. 3.

Object	Coordinates	Weights
Shell	(-100.0,0.0,0.0)	1.0
	(-100.0,100.0,0.0)	0.707107
	(0.0,100.0,0.0)	1.0
	(100.0,100.0,0.0)	0.707107
	(100.0,0.0,0.0)	1.0
	(-100.0,0.0,100.0)	1.0
	(-100.0,100.0,100.0)	0.707107
	(0.0,100.0,100.0)	1.0
	(100.0,100.0,100.0)	0.707107
	(100.0,0.0,100.0)	1.0
	(-100.0,0.0,200.0)	1.0
	(-100.0,100.0,200.0)	0.707107
	(0.0,100.0,200.0)	1.0
	(100.0,100.0,200.0)	0.707107
	(100.0,0.0,200.0)	1.0

(continued on next page)

Table 7 shows that the frequencies and the mode shapes from IGA method are in good agreement with those from Nastran simulation. It can be concluded that the IGA method can solve the free vibration problem correctly.

Then, to study the effect of the shell thickness and the boundary condition on natural frequency, the first three orders frequencies $\omega_1, \omega_2, \omega_3$ are calculated. During the analysis, the geometry and material parameters are all unchanged except for the shell thickness. Considering both clamped and simply supported stiffened shallow shell, we can see that the larger the shell thickness is, the greater the frequency will be, as shown in Fig. 8. Besides, the natural frequencies got from clamped stiffened shallow shell are higher than those of simply supported one.

5. Conclusions

This paper proposed an efficient isogeometric analysis method to analyze the free vibration of curvilinearly stiffened cylindrical and shallow shells. In the process of establishing formulation, an interpolation function matrix was introduced which solved the coupling issue of the shell and stiffener. During the analysis of some examples, we mainly investigated the following cases. First of all, the number of shell elements and stiffener elements was changed, and we finally got an optimal number of elements as well as stable and convergence natural frequencies with good accuracy. Then, different kinds of ply modes of the stiffeners are considered. From the third example, it is found that ply modes of the stiffeners have a little effect on the natural frequencies and mode shapes. Thirdly, the influence of the shell thickness and boundary conditions was studied. The results showed that with the increase of the shell thickness, the evident increment of the natural frequencies could be observed. Besides, boundary conditions have some effects on the natural frequencies too. So, altering the shell thickness and boundary condition can obtain ideal structural vibration frequencies and modes. The corresponding results of these examples were compared with those of Nastran and other numerical methods so that the correctness of the present method could be verified.

Acknowledgements

This work is supported by the National Natural Science Foundation of China (11272054, 11672038).

Table 8 (continued)

Object	Coordinates	Weights
Beam	(−100.0,0.0,300.0)	1.0
	(−100.0,100.0,300.0)	0.707107
	(0.0,100.0,300.0)	1.0
	(100.0,100.0,300.0)	0.707107
	(100.0,0.0,300.0)	1.0
	(−100.0,0.0,400.0)	1.0
	(−100.0,100.0,400.0)	0.707107
	(0.0,100.0,400.0)	1.0
	(100.0,100.0,400.0)	0.707107
	(100.0,0.0,400.0)	1.0
	(−100.0,300.0,0.0)	1.0
	(−90.0969,262.3490,43.3884)	1.0
	(−62.3490,177.7479,78.1831)	1.0
	(−22.2521,109.9031,97.4928)	1.0
	(22.2521,109.9031,97.4928)	1.0
	(62.3490,177.7479,78.1831)	1.0
	(−90.0969,262.3490,43.3884)	1.0
	(100.0,300.0,0.0)	1.0

Appendix B

The two initial shell element knot vectors (one for each direction) are both {0, 0, 0, 0, 0, 1, 1, 1, 1, 1}. The initial knot vector of the stiffener is {0, 0, 0, 0.25, 0.5, 0.75, 1, 1, 1, 1}. The initial control points and weights are listed in Table 9.

Table 9

The coordinates of control points and weights in Fig. 5.

Object	Coordinates	Weights
Shell	(−100.0,0.0,0.0)	1.0
	(−100.0,100.0,0.0)	0.707107
	(0.0,100.0,0.0)	1.0
	(100.0,100.0,0.0)	0.707107
	(100.0,0.0,0.0)	1.0
	(−100.0,0.0,50.0)	1.0
	(−100.0,100.0,50.0)	0.707107
	(0.0,100.0,50.0)	1.0
	(100.0,100.0,50.0)	0.707107
	(100.0,0.0,50.0)	1.0
	(−100.0,0.0,100.0)	1.0
	(−100.0,100.0,100.0)	0.707107
	(0.0,100.0,100.0)	1.0
	(100.0,100.0,100.0)	0.707107
	(100.0,0.0,100.0)	1.0
	(−100.0,0.0,150.0)	1.0
	(−100.0,100.0,150.0)	0.707107
	(0.0,100.0,150.0)	1.0
	(100.0,100.0,150.0)	0.707107
	(100.0,0.0,150.0)	1.0
	(−100.0,0.0,200.0)	1.0
	(−100.0,100.0,200.0)	0.707107
	(0.0,100.0,200.0)	1.0
	(100.0,100.0,200.0)	0.707107
	(100.0,0.0,200.0)	1.0
Beam	(−100.0,183.3333,0.0)	1.0
	(−98.7688,182.0251,15.6434)	1.0
	(−95.1057,178.1925,30.9017)	1.0
	(−89.1007,172.1033,45.3990)	1.0
	(−80.9017,164.1776,58.7785)	1.0
	(−70.7107,154.9509,70.7107)	1.0
	(−58.7785,145.0278,80.9017)	1.0
	(−45.3990,135.0299,89.1007)	1.0
	(−30.9017,125.5437,95.1057)	1.0
	(−15.6434,117.0731,98.7688)	1.0
	(0.0,110.0,100.0)	1.0
	(15.6434,104.5583,98.7688)	1.0
	(30.9017,100.8224,95.1057)	1.0
	(45.3990,98.7106,89.1007)	1.0
	(58.7785,98.0050,80.9017)	1.0

(continued on next page)

Table 9 (continued)

Object	Coordinates	Weights
	(70.7107,98.3824,70.7107)	1.0
	(80.9017,99.4563,58.7785)	1.0
	(89.1007,100.8228,45.3990)	1.0
	(95.1057,102.1080,30.9017)	1.0
	(98.7688,103.0101,15.6434)	1.0
	(100.0,103.3333,0.0)	1.0
	(−100.0,65.0,0.0)	1.0
	(−98.7688,65.3656,15.6434)	1.0
	(−95.1057,66.4084,30.9017)	1.0
	(−89.1007,67.9728,45.3990)	1.0
	(−80.9017,69.8176,58.7785)	1.0
	(−70.7107,71.6421,70.7107)	1.0
	(−58.7785,73.1184,80.9017)	1.0
	(−45.3990,73.9271,89.1007)	1.0
	(−30.9017,73.7931,95.1057)	1.0
	(−15.6434,72.5169,98.7688)	1.0
	(0.0,70.0,100.0)	1.0
	(15.6434,66.2595,98.7688)	1.0
	(30.9017,61.4324,95.1057)	1.0
	(45.3990,55.7675,89.1007)	1.0
	(58.7785,49.6070,80.9017)	1.0
	(70.7107,43.3579,70.7107)	1.0
	(80.9017,37.4569,58.7785)	1.0
	(89.1007,32.3326,45.3990)	1.0
	(95.1057,28.3662,30.9017)	1.0
	(98.7688,25.8580,15.6434)	1.0
	(100.0,25.0,0.0)	1.0
	(−100.0,15.7143,0.0)	1.0
	(−98.7688,17.0488,15.6434)	1.0
	(−95.1057,20.9939,30.9017)	1.0
	(−89.1007,27.3782,45.3990)	1.0
	(−80.9017,35.9285,58.7785)	1.0
	(−70.7107,46.2886,70.7107)	1.0
	(−58.7785,58.0416,80.9017)	1.0
	(−45.3990,70.7364,89.1007)	1.0
	(−30.9017,83.9145,95.1057)	1.0
	(−15.6434,97.1356,98.7688)	1.0
	(0.0,110.0,100.0)	1.0
	(15.6434,122.1652,98.7688)	1.0
	(30.9017,133.3572,95.1057)	1.0
	(45.3990,143.3748,89.1007)	1.0
	(58.7785,152.0872,80.9017)	1.0
	(70.7107,159.4256,70.7107)	1.0
	(80.9017,165.3712,58.7785)	1.0
	(89.1007,169.9392,45.3990)	1.0
	(95.1057,173.1630,30.9017)	1.0
	(98.7688,175.0789,15.6434)	1.0
	(100.0175,7143,0.0)	1.0

Appendix C

The two initial shell element knot vectors (one for each direction) are both $\{0, 0, 0, 1, 1, 1\}$. The initial knot vector of the stiffener is $\{0, 0, 0, 0, 0.25, 0.5, 0.75, 1, 1, 1, 1\}$. The initial control points and weights are listed in Table 10.

Table 10
The coordinates of control points and weights in Fig. 7.

Object	Coordinates	Weights
Shell	(−784.9, −784.9, 242.5465)	1.0
	(0.0, −784.9, 0.0)	1.0
	(784.9, −784.9, 242.5465)	1.0
	(−784.9, 0.0, 0.0)	1.0
	(0.0, 0.0, −242.5465)	1.0
	(784.9, 0.0, 0.0)	1.0
	(−784.9, 784.9, 242.5465)	1.0
	(0.0, 784.9, 0.0)	1.0
	(784.9, 784.9, 242.5465)	1.0

(continued on next page)

Table 10 (continued)

Object	Coordinates	Weights
Beam	(−784.9, 9.2244, 121.2900)	1.0
	(−523.2667, 8.0583, 53.9120)	1.0
	(−261.6333, 6.3958, 13.4829)	1.0
	(0.0, 0.0, 0.0)	1.0
	(261.6333, −6.3958, 13.4829)	1.0
	(523.2667, −8.0583, 53.9120)	1.0
	(784.9, −9.2244, 121.2900)	1.0

References

- [1] W.H. Hoppmann, Orthogonally stiffened plates, 1953, TR-8B.
- [2] A.J. Stanley, N. Ganesan, Free vibration characteristics of stiffened cylindrical shells, *Comput. Struct.* 65 (1997) 33–45.
- [3] A. Nayak, J. Bandyopadhyay, On the free vibration of stiffened shallow shells, *J. Sound Vib.* 255 (2002) 357–382.
- [4] A. Samanta, M. Mukhopadhyay, Free vibration analysis of stiffened shells by the finite element technique, *Eur. J. Mech.-A/Solids* 23 (2004) 159–179.
- [5] Z. Pan, X. Li, J. Ma, A study on free vibration of a ring-stiffened thin circular cylindrical shell with arbitrary boundary conditions, *J. Sound Vib.* 314 (2008) 330–342.
- [6] B. Efimtsov, L. Lazarev, Forced vibrations of plates and cylindrical shells with regular orthogonal system of stiffeners, *J. Sound Vib.* 327 (2009) 41–54.
- [7] V. Balamurugan, S. Narayanan, Finite element modeling of stiffened piezolaminated plates and shells with piezoelectric layers for active vibration control, *Smart Mater. Struct.* 19 (2010) 533–536.
- [8] P. Shi, R.K. Kapania, C.Y. Dong, Finite element approach to the static, vibration and buckling analysis of curvilinearly stiffened plates. in: *Proceedings of the 56th AIAA/ASCE/AHS/ASC Structures, Structural Dynamics, and Materials Conference*, AIAA J., 2015.
- [9] P. Shi, R.K. Kapania, C.Y. Dong, Free vibration of curvilinearly stiffened cylindrical shells. in: *Proceedings of the 56th AIAA/ASCE/AHS/ASC Structures, Structural Dynamics, and Materials Conference*, AIAA J., 2015.
- [10] W. Zhao, R.K. Kapania, Buckling analysis of unitized curvilinearly stiffened composite panels, *Compos. Struct.* 135 (2016) 365–382.
- [11] L.Y. Li, Perturbation solution for the free vibration of Ring-stiffened cylindrical shells, *Appl. Math. Mech.* 3 (1987) 283–292.
- [12] S.P. Cheng, C. Dade, Dynamic analysis of stiffened plates and shells using spline gauss collocation method, *Comput. Struct.* 36 (1990) 623–629.
- [13] B. Mustafa, R. Ali, An energy method for free vibration analysis of stiffened circular cylindrical shells, *Comput. Struct.* 32 (1989) 355–363.
- [14] P. Shi, R.K. Kapania, C.Y. Dong, Free vibration of curvilinearly stiffened shallow shells, *J. Vib. Acoust.* 137 (2013) 1–15.
- [15] A. Jafari, M. Bagheri, Free vibration of non-uniformly ring stiffened cylindrical shells using analytical, experimental and numerical methods, *Thin-Walled Struct.* 44 (2006) 82–90.
- [16] Y. Qu, Y. Chen, X. Long, H. Hua, G. Meng, A modified variational approach for vibration analysis of ring-stiffened conical–cylindrical shell combinations, *Eur. J. Mech.-A/Solids* 37 (2013) 200–215.
- [17] T.J.R. Hughes, J.A. Cottrell, Y. Bazilevs, Isogeometric analysis: CAD, finite elements, NURBS, exact geometry and mesh refinement, *Comput. Methods Appl. Mech. Eng.* 194 (2005) 4135–4195.
- [18] I. Akkerman, Y. Bazilevs, V.M. Calo, T.J.R. Hughes, S. Hulshoff, The role of continuity in residual-based variational multiscale modeling of turbulence, *Comput. Mech.* 41 (2008) 371–378.
- [19] Y. Bazilevs, V.M. Calo, J.A. Cottrell, T.J.R. Hughes, A. Reali, G. Scovazzi, Variational multiscale residual-based turbulence modeling for large eddy simulation of incompressible flows, *Comput. Methods Appl. Mech. Eng.* 197 (2007) 173–201.
- [20] Y. Bazilevs, I. Akkerman, Large eddy simulation of turbulent Taylor-Couette flow using isogeometric analysis and the residual-based variational multiscale method, *J. Comput. Phys.* 229 (2010) 3402–3414.
- [21] Y. Bazilevs, V.M. Calo, Y. Zhang, T.J.R. Hughes, Isogeometric fluid–structure interaction analysis with application to arterial blood flow, *Comput. Mech.* 38 (2006) 310–322.
- [22] Y. Bazilevs, V.M. Calo, T.J.R. Hughes, Y. Zhang, Isogeometric fluid–structure interaction: theory, algorithms and computations, *Comput. Mech.* 43 (2008) 3–37.
- [23] Y. Zhang, Y. Bazilevs, S. Goswami, C. Bajaj, T.J.R. Hughes, Patient-specific vascular NURBS modeling for isogeometric analysis of blood flow, *Comput. Methods Appl. Mech. Eng.* 196 (2007) 2943–2959.
- [24] F. Auricchio, L.B. da Veiga, C. Lovadina, A. Reali, The importance of the exact satisfaction of the incompressibility constraint in nonlinear elasticity: mixed fems versus NURBS-based approximations, *Comput. Methods Appl. Mech. Eng.* 199 (2010) 314–323.
- [25] F. Auricchio, L.B. da Veiga, A. Buffa, C. Lovadina, A. Reali, G. Sangalli, A fully ‘locking-free’ isogeometric approach for plane linear elasticity problems: a stream function formulation, *Comput. Methods Appl. Mech. Eng.* 197 (2007) 160–172.
- [26] T. Elguedj, Y. Bazilevs, V.M. Calo, T.J.R. Hughes, B⁺ and F⁺ projection methods for nearly incompressible linear and non-linear elasticity and plasticity using higher-order NURBS elements, *Comput. Methods Appl. Mech. Eng.* 197 (2008) 2732–2762.
- [27] J.A. Cottrell, T.J.R. Hughes, A. Reali, Studies of refinement and continuity in isogeometric structural analysis, *Comput. Methods Appl. Mech. Eng.* 196 (2007) 4160–4183.
- [28] J.A. Cottrell, A. Reali, Y. Bazilevs, T.J.R. Hughes, Isogeometric analysis of structural vibrations, *Comput. Methods Appl. Mech. Eng.* 195 (2006) 5257–5296.
- [29] D.J. Bensen, Y. Bazilevs, M.C. Hsu, T.J.R. Hughes, Isogeometric shell analysis: the Reissner-Mindlin shell, *Comput. Methods Appl. Mech. Eng.* 199 (2009) 276–289.
- [30] H. Gomez, V.M. Calo, Y. Bazilevs, T.J.R. Hughes, Isogeometric analysis of the Cahn-Hilliard phase-field model, *Comput. Methods Appl. Mech. Eng.* 197 (2008) 4333–4352.
- [31] H. Chien, H. Thai, N. Nguyen-Xuan, N. Nguyen-Thanh, T.-H. Le, T. Nguyen-Thoi, T. Rabczuk, Static, free vibration, and buckling analysis of laminated composite Mindlin-Reissner plates using NURBS-based isogeometric approach, *Int. J. Numer. Methods Eng.* 91 (2012) 571–603.
- [32] J. Kiendl, K.U. Bletzinger, J. Linhard, R. Wuchner, Isogeometric shell analysis with Kirchhoff-Love elements, *Comput. Methods Appl. Mech. Eng.* 198 (2009) 3902–3914.
- [33] N. Nguyen-Thanh, J. Kiendl, H. Nguyen-Xuan, R. Wuchner, K.U. Bletzinger, Y. YBazilevs, T. Rabczuk, Rotation free isogeometric thin shell analysis using PHT-splines, *Comput. Methods Appl. Mech. Eng.* 200 (2011) 3410–3424.
- [34] J. Kiendl, Y. Bazilevs, M.C. Hsu, R. Wchnr, K.U. Bletzinger, The bending strip method for isogeometric analysis of Kirchhoff-Love shell structures comprised of multiple patches, *Comput. Methods Appl. Mech. Eng.* 199 (2010) 2403–2416.
- [35] D.J. Benson, Y. Bazilevs, M.C. Hsu, T.J.R. Hughes, A large deformation, rotation-free, isogeometric shell, *Comput. Methods Appl. Mech. Eng.* 200 (2011) 1367–1378.
- [36] W.A. Wall, M.A. Frenzel, C. Cyron, Isogeometric structural shape optimization, *Comput. Methods Appl. Mech. Eng.* 197 (2008) 2976–2988.
- [37] V.P. Nguyen, R.N. Simpsona, S.P.A. Bordas, T. Rabczuk, Isogeometric analysis : a review and computer implementation aspects, *Math. Comput. Simul.* 117 (2015) 89–116.
- [38] M.M. Lipschutz, *Schaum's Outline of Theory and Problems of Differential Geometry*, McGraw-Hill, New York, 1969.